Mechanisms of Development 122 (2005) 131–144

www.elsevier.com/locate/modo

The T-box transcription factor *Tbx15* is required for skeletal development

Manvendra K. Singh[a], Marianne Petry[a], Bénédicte Haenig[b,1], Birgit Lescher[b], Michael Leitges[b,2], Andreas Kispert[a,b,*]

[a]*Institut für Molekularbiologie, OE5250, Medizinische Hochschule Hannover, Carl-Neuberg-Str. 1, 30625 Hannover, Germany*
[b]*Max-Planck-Institut für Immunbiologie, Stübeweg 51, 79108 Freiburg, Germany*

Received 30 July 2004; received in revised form 24 October 2004; accepted 25 October 2004
Available online 23 November 2004

Abstract

During early limb development several signaling centers coordinate limb bud outgrowth as well as patterning. Members of the T-box gene family of transcriptional regulators are crucial players in these processes by activating and interpreting these signaling pathways. Here, we show that *Tbx15*, a member of this gene family, is expressed during limb development, first in the mesenchyme of the early limb bud, then during early endochondral bone development in prehypertrophic chondrocytes of cartilaginous templates. Expression is also found in mesenchymal precursor cells and prehypertrophic chondrocytes, respectively, during development of skeletal elements of the vertebral column and the head. Analysis of *Tbx15* null mutant mice indicates a role of *Tbx15* in the development of skeletal elements throughout the body. Mutants display a general reduction of bone size and changes of bone shape. In the forelimb skeleton, the scapula lacks the central region of the blade. Cartilaginous templates are already reduced in size and show a transient delay in ossification in mutant embryos. Mutants show a significantly reduced proliferation of prehypertrophic chondrocytes as well as of mesenchymal precursor cells. These data suggest that *Tbx15* plays an important role in the development of the skeleton of the limb, vertebral column and head by controlling the number of mesenchymal precursor cells and chondrocytes.

Keywords: Limb; Skeleton; Chondrocyte; T-box; Proliferation

1. Introduction

The vertebrate limb has long been employed as a model system to analyze the molecular pathways underlying both patterning as well as cellular differentiation during skeletal development. Limb development starts with the thickening of the lateral plate mesoderm and the formation of limb buds at the flanks of the early organogenesis stage embryo. Mesenchymal cells of the bud will give rise to all the progenitors of the skeletal system as well as to tendons and muscle sheaths. Skeletogenesis starts with the aggregation and condensation of mesenchymal precursor cells to templates that prefigure the shape of the future bones at their appropriate position. Development proceeds by endochondral ossification via a cartilaginous intermediate, a process that contrasts with the direct (intramembranous) ossification of some bones of the skull and the clavicle. Patterning of individual skeletal elements occurs at the level of the condensation, i.e. the number and adhesion properties of mesenchymal cells regulate the size and shape of the future bone. Experimental manipulations primarily done in chick embryos and genetic experiments in the mouse have provided evidence that specific regions of the early limb bud act as signaling centers that regulate limb skeletal patterning along the proximal–distal (PD), the anterior–posterior (AP) and the dorso-ventral (DV) limb axes. Patterning is subsequently refined by the combinatorial action of various classes of transcription factors including *Hox* genes (for recent reviews on limb and skeletal patterning see Karsenty

* Corresponding author. Address: Institut für Molekularbiologie, OE5250, Medizinische Hochschule Hannover, Carl-Neuberg-Str. 1, 30625 Hannover, Germany. Tel.: +49 511 532 4017; fax: +49 511 532 4283.
E-mail address: kispert.andreas@mh-hannover.de (A. Kispert).
[1] Present address: Actelion Pharmaceuticals, Gewerbestr. 16, 4123 Allschwil, Switzerland.
[2] Present address: Max-Planck-Institut für Experimentelle Endokrinologie, Feodor-Lynen-Str. 7, 30625 Hannover, Germany.

0925-4773/$ - see front matter © 2004 Elsevier Ireland Ltd. All rights reserved.
doi:10.1016/j.mod.2004.10.011

and Wagner, 2002; Kronenberg, 2003; Niswander, 2003; Mariani and Martin, 2003; Tickle, 2003).

T-box (*Tbx*) genes constitute a multigene family encoding transcription factors characterized by a highly conserved DNA-binding region, the T-box. T-box genes play crucial roles in the development of diverse tissues and organs both in vertebrates and in invertebrates (Papaioannou, 2001). Analyses both in chick and in mouse suggest that at least seven *Tbx* family members are important regulators of limb development. *Tbx5* and *Tbx4* are a closely related pair of T-box genes with differential expression in the developing forelimb and hindlimb buds, respectively (Gibson-Brown et al., 1996). Mutations in human *TBX5* underlie a developmental disorder, Holt-Oram syndrome, where heterozygous carriers show heart and upper limb defects (Li et al., 1997). Misexpression experiments in chick embryos suggest a role for either factor in specifying forelimb and hindlimb identity, respectively (Rodriguez Esteban et al., 1999; Takeuchi et al., 1999). Loss of function studies in the mouse have precluded a direct analysis of such a role but have instead revealed a requirement for *Tbx4* and *Tbx5* in triggering limb outgrowth. Here, *Tbx4* and *Tbx5* appear to coordinate Wnt and FGF signaling between limb mesenchyme and the overlying ridge ectoderm (Naiche and Papaioannou, 2003; Rallis et al., 2003; Takeuchi et al., 2003).

Brachyury (*T*), the prototypical member of the *Tbx* gene family was recently found to play an important role in maintaining the AER. Expression of *T* in the lateral plate mesoderm and later in the mesoderm underlying the AER might put *T* in a regulatory loop of Wnt and FGF signaling between the ridge epithelium and the subridge mesenchyme involved in maintaining a functional AER (Liu et al., 2003).

Tbx2 and *Tbx3* form a second pair of structurally related T-box genes with an important function in limb patterning. *Tbx2* and *Tbx3* are expressed in anterior and posterior edges of limb buds with distinct domains in relation to posterior digit identity (Gibson-Brown et al., 1996). Mutations in human *TBX3* have been found to cause ulnar-mammary syndrome, a condition characterized by absence or deformation of the ulna and posterior digits IV and V (Bamshad et al., 1997). Mice homozygous for a targeted null mutation of *Tbx3* show severe malformation of both forelimbs and hindlimbs characterized by AP-patterning defects (Davenport et al., 2003). Recent misexpression experiments in chick further support a role for *Tbx2* and *Tbx3* in anterior–posterior limb patterning, namely specification of identity of digits III and IV. These experiments suggest feedback and feedforward loops between Tbx2/3 and Shh and BMP signaling cascades to specify posterior digit identity (Suzuki et al., 2004).

Tbx18 and *Tbx15* constitute a third pair of closely related T-box genes expressed during limb development. *Tbx18* is expressed in the proximal region of the limb bud mesenchyme (Kraus et al., 2001). *Tbx18*$^{-/-}$ mice do not show morphological defects in the limbs but exhibit severe malformation of the vertebral column, a phenotype that was traced back to defects in AP-somite polarization (Bussen et al., 2004).

Expression of *Tbx15* (also referred to as *Tbx8* or *Tbx14*; NCBI GeneBank) has been reported in limb buds, in the craniofacial region and in the skin during mouse development (Agulnik et al., 1998; Candille et al., 2004). Analyses of the *droopy ear* mouse mutation, in which *Tbx15* is deleted, and of a targeted null allele of *Tbx15* have revealed a role for *Tbx15* in DV-patterning of the mouse coat (Curry, 1959; Candille et al., 2004). Here, we extend the analysis of the *Tbx15* skeletal phenotype (Curry, 1959), and show that *Tbx15* is dynamically expressed in the developing limb bud as well as in other regions of the embryo associated with mesenchymal condensations during early endochondral bone formation. In mice lacking *Tbx15* most bones of the appendicular skeleton and the upper vertebral column, and some of the skull are reduced in size, and show subtle changes in shape. The scapula is marked by a hole in the center of the blade. Defects in the adult skeleton can be traced to changes in the mesenchymal and cartilaginous anlagen of the skeleton, and may be caused by a reduced proliferation of mesenchymal precursor cells and prehypertrophic chondrocytes.

2. Results

2.1. Expression of Tbx15 in limb and skeletal development

Previous studies described *Tbx15* expression in early limb buds, branchial arches, flanks and the craniofacial region by whole-mount in situ hybridization, and in skin development using section in situ hybridization analysis (Agulnik et al., 1998; Candille et al., 2004). In order to investigate expression in (skeletal) development of limbs in more detail, we hybridized whole embryos from embryonic day (E) 8.5 to 12.5 and sections of whole embryos and individual bones from E10.5 to 18.5 with an antisense riboprobe derived from a full length *Tbx15* cDNA (Fig. 1).

Tbx15 expression is prominent in limb development from E9.0 to 16.5 (Fig. 1A–D,F,H,I,K,L,O–R). Expression is first seen in the developing forelimb buds on E9.0–9.5 (Fig. 1A). On E10.5, expression is found along the proximo-distal extension in the central region of the forelimb buds but not in the anterior and posterior edges (Fig. 1B with inset). This pattern is maintained throughout further limb development (Fig. 1C,D). With formation of digits expression is confined to digits II–IV (Figs. 1P,2Dc). Hindlimb expression follows that of the forelimb buds with a developmental delay of one day (Fig. 1B–D). Section in situ hybridization analysis revealed that expression is confined to the mesenchymal compartment of the developing limb buds. On E10.5, expression is highest in the central core of the forelimb bud (Fig. 1F). With formation of a mesenchymal preskeleton, expression becomes weaker in the condensing cells but is

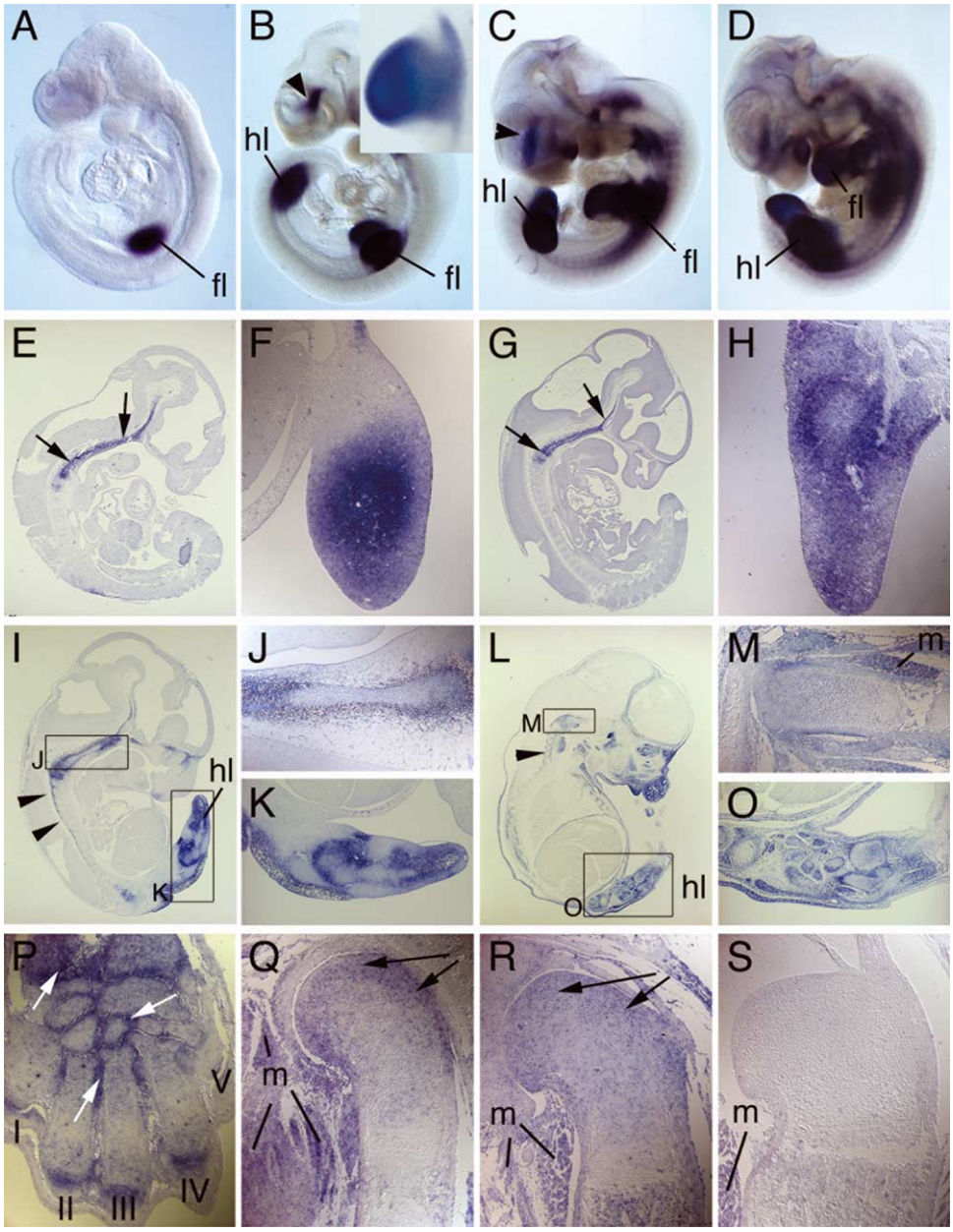

Fig. 1. Expression of *Tbx15* in limb and skeletal development. (A–D) In situ hybridization analysis of *Tbx15* expression in whole embryos at E9.5 (A), E10.5 with inset of a forelimb bud (B), E11.5 (C) and E12.0 (D). Arrowheads in (B,C) point to an expression domain above the eye. (E–S) Section in situ hybridization analysis of *Tbx15* expression at E10.5 (E,F), E11.5 (G,H), E12.5 (I–K), E14.5 (L–O), E15.5 (P,Q), E16.5 (R), E18.5 (S). (E,G,I,L) Sagital sections of whole embryos, anterior is up. Arrows (in E,G) point to head mesenchyme. (F,H) Higher magnification of transverse sections of forelimb buds, proximal is up. (K,O) Higher magnification of hindlimb buds, proximal is to the left. (J,M) Higher magnification of the cartilage primordium of the basioccipital bone. (P–S) *Tbx15* expression in endochondral bone development. (P) Arrows point to strong *Tbx15* expression in the mesenchyme surrounding the developing bones of the hand plate and digits. Digits are labeled I–V. (Q,R) Arrows point to *Tbx15* expression in the resting chondrocytes of the proximal region of the humerus. (S) Absence of *Tbx15* expression in the humerus. fl, forelimb bud; hl, hindlimb bud; m, muscle.

maintained at a high level in the surrounding mesenchyme (Fig. 1H,K,O). Cartilage formation starts on E12.5–13 in the region of the future humerus. From this time on, *Tbx15* expression is high in the developing joints, the articular mesenchyme and the perichondrium (Fig. 1L,O, arrows in P). Within the cartilaginous templates of limb bones, *Tbx15* expression is detected in the resting and proliferating, i.e. prehypertrophic chondrocytes, but is downregulated upon hypertrophy (Fig. 1P–R, arrows in Q,R for expression in resting chondrocytes). Expression in the humerus fails to be detected after E16.5 (Fig. 1S).

Section in situ analysis revealed that *Tbx15* expression is also associated with the development of the skeleton of the skull and the vertebral column (Fig. 1E,G,I,J,L,M). On E10.5, *Tbx15* is highly expressed in the unsegmented cranial mesenchyme (arrows in Fig. 1E). Expression is maintained

on E11.5 (arrows in Fig. 1G) but is downregulated upon condensation of mesenchymal cells into the primordia of the skeletal elements on E12.5 (Fig. 1I,J for the mesenchymal primordium of the basioccipital bone). Similar to the situation in endochondral development of limb bones, high *Tbx15* expression is maintained in mesenchymal cells surrounding the condensations, whereas resting and proliferating chondrocytes show lower expression (Fig. 1M). From E12.5 to 14.5, mesenchymal cells surrounding the condensations of the vertebral bodies of the vertebral column also express high levels of *Tbx15* (arrowheads in Fig. 1I,L).

Expression in supraocular mesenchyme starting form E10.5 suggests that *Tbx15* expression is also associated with the mesenchymal primordia of bones undergoing intramembranous ossification (arrowheads in Fig. 1B,C). From E13.5 onwards, *Tbx15* expression is also found in the skeletal musculature (see muscles (m) in Fig. 1M,Q,R,S).

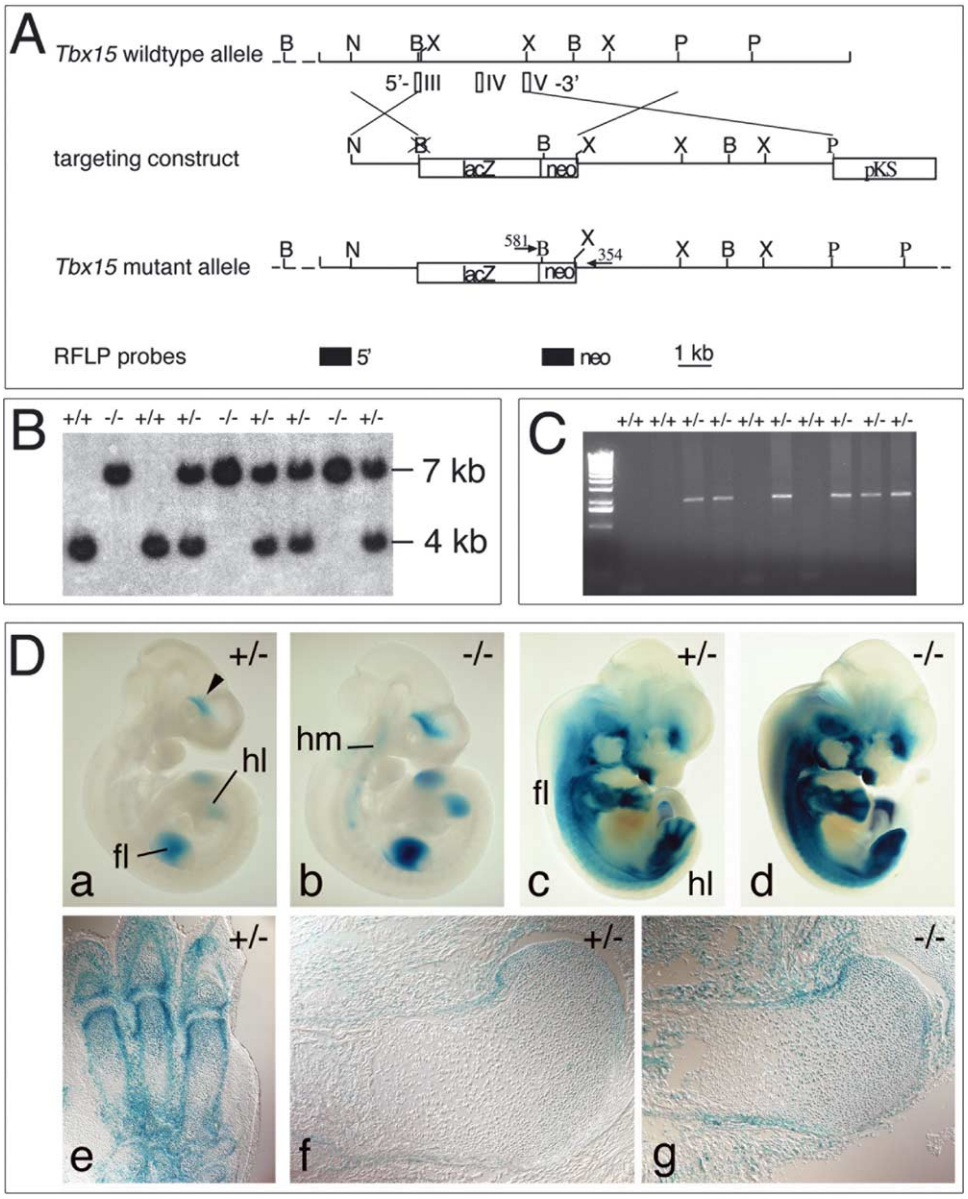

Fig. 2. Targeted disruption of the *Tbx15* locus. (A) Schematic representation of the targeting strategy. Restriction map of the wildtype locus with white boxes representing exons III–V of *Tbx15*. Arrows show location and orientation of PCR primers. Fragments used as RFLP probes are shown. The fragment designated as 5′ detects the *Bam*HI-RFLP shown in (B). B, *Bam*HI; N, *Not*I; P, *Pst*I; X, *Xho*I; lacZ, *lacZ* gene encoding β-galactosidase; neo, loxP-flanked *neomycin* selection cassette. (B) Southern blot analysis of *Bam*HI-digested genomic DNA extracted from E18.5 embryos derived from intercrosses of *Tbx15*/+ mice. Genotypes are indicated above each lane. The 4 and 7 kbp band represent the wildtype and the mutant allele, respectively. (C) PCR genotyping of mice from matings of heterozygous males with wildtype females using primers specific for the mutant allele. The genotypes are indicated above each lane. (D) β-Galactosidase assay to test for *lacZ* expression in heterozygous and homozygous *Tbx15* mutant embryos. Whole embryos at E10.5 (a,b) and E12.5 (c,d), fl, forelimb bud; hl, hindlimb bud; hm, head mesenchyme. Sections of a hand plate of a heterozygous *Tbx15* embryo at E15.5 (e), and of the proximal part of a humerus at E16.5 (f,g). Genotypes are indicated in the figure.

2.2. Targeted disruption of the Tbx15 gene

To elucidate the role of *Tbx15* in limb and skeletal development we generated mice deficient for the *Tbx15* gene (Fig. 2). Insertion of a lacZ-loxP-flanked-neo-cassette into exon3 of the *Tbx15* locus leads to a truncation of the open reading frame early in the T-box domain resulting in a functional null allele. The *lacZ* gene was inserted in frame into the coding region to visualize endogenous *Tbx15* expression from the mutated allele by β-galactosidase activity staining (Fig. 2A,D). The β-galactosidase activity pattern both in heterozygous and in homozygous *Tbx15* mutant embryos faithfully reflects *Tbx15* expression at all stages analyzed (Fig. 2D). β-Galactosidase activity is nuclear suggesting that the 154 N-terminal amino acid residues of the Tbx15 protein harbor a nuclear localization signal.

2.3. External morphology and skeletal malformations of $Tbx15^{-/-}$ mice

Mice heterozygous for the mutant *Tbx15* allele appear normal and are fertile. In contrast, no viable homozygotes were recovered from heterozygous intercrosses at 2 weeks of age (>200 offspring). However, homozygotes were observed at the expected Mendelian ratio from E10 to 18 as well as shortly after birth (data not shown). Mutant pups that are characterized by a thinner body die within one or two days after birth most likely because they cannot compete with their wildtype littermates for milk. When phenotypically normal littermates were removed (except one or two to serve as controls) most of the mutant pups survived and reached adulthood. After weaning $Tbx15^{-/-}$ mice did not show any lethality. However, they exhibited reduced fertility and bad nursing behavior making it difficult to rederive homozygotes from homozygous intercrosses. $Tbx15^{-/-}$ mice are distinguished by multiple morphological defects from wildtype or heterozygous animals. Mutant mice are shorter and leaner than their control littermates even when they reach one year of age. They show craniofacial abnormalities including widely spaced eyes, a broad nasal area and abnormal position of the ears. On an *agouti* background, $Tbx15^{-/-}$ mice are easily recognized by a dorsal expansion of the lighter hair of the belly region. *Tbx15* mice seem to have normally differentiated skeletal muscles but a reduced total muscle mass (data not shown).

Skeletal preparations ($n=6$ each for wildtype and mutants) revealed malformations of the appendicular skeleton, skull and vertebral column (Fig. 3Ab). Skeletons of adult $Tbx15^{-/-}$ mice are characterized by a general reduction of bone size, widespread but subtle changes of bone shape, and poor articulations. Within the appendicular skeleton the pectoral girdle and the forelimbs are most strongly affected (Fig. 3B). The mutant scapula is small and distinguished by a hole in the posterior half (arrow in Fig. 3Bb). Spine, acromion and clavicle are reduced in size (Fig. 3Bd,h). The humerus is short; radius and ulna are sometimes twisted (Fig. 3Bb,f). The length of metacarpals and phalanges is slightly reduced (Fig. 3Bb). The pelvic region and the hindlimbs are less severely affected in $Tbx15^{-/-}$ mice (Fig. 3Cb,d). Strong length reduction is, however, seen in the femur and the metatarsals (Fig. 3Cf,h).

In the vertebral column specific malformations are seen in the atlas (Fig. 3Db), the axis (Fig. 3Dd) and the second thoracic vertebra, where the spinal process is largely reduced (Fig. 3Df).

In the head, many bones show subtle changes in size and shape (Fig. 3E, see e.g. Fig. 3Ec,d for the frontal and parietal bones). Most strikingly, the foramen magnum (arrow in Fig. 3Ef) is much reduced in size due to a vertical displacement of the supraoccipital bone and a smaller basioccipital bone (Fig. 3Eb,f). In the squamosum, the glenoid and caudal processes are fused into a bony mass (white outline in Fig. 3Eb). Thus, bones formed by desmal and by endochondral ossification, respectively, are affected in the head skeleton.

2.4. Skeletal defects in $Tbx15^{-/-}$ embryos arise early in development

To evaluate the developmental onset of specific defects in the skeleton in $Tbx15^{-/-}$ embryos, alcian blue/alizarin red and alizarin blue preparations of skeletons of mutant embryos and wildtype littermates were made at E18.5 ($n=14$) and E13.5 ($n=6$), respectively (Fig. 4). At E18.5, the skeletal changes of adult $Tbx15^{-/-}$ mice are already forecast. In the pectoral girdle of the mutant, the scapula is smaller and shows an oval hole in the posterior half (arrow in Fig. 4Ag), acromion and spine are reduced in size and not yet ossified (a in inset in Fig. 4Ag). The humerus is shorter and thinner and the deltoid ridge less pronounced than in the wildtype. Radius and ulna are also reduced in length (Fig. 4Ag). The vertebral column of wildtype embryos shows a clear S-bend in the cervical and thoracic region on E18.5 (Fig. 4Ac). In the mutant, the vertebral column is rather straight positioning skull and vertebral column perpendicular to each other (Fig. 4Ah). The vertebral bodies of the atlas and axis are fused in the wildtype but remain separate in the mutant (arrowhead in Fig. 4Ah). The ventral extension of the atlas, the dens, is split into two parts in the mutant with the upper part getting incorporated in the basioccipital bone (arrow in Fig. 4Ah). Atlas and axis are smaller than in the wildtype (Fig. 4Ah). The glenoid process of the squamosum is widened, supra and lateral occipitals are prematurely fused in the head skeleton (data not shown). The basioccipital bone is extended posteriorly; the foramen magnum is reduced (arrow in Fig. 4Ai). The parietal and frontal bones are still widely separated leaving a wide dorsal opening at this point (dotted white lines in Fig. 4Aj).

Most of the defects described in the E18.5 mutant skeleton are already apparent in the cartilaginous preskeleton of $Tbx15^{-/-}$ embryos at E13.5 (Fig. 4B).

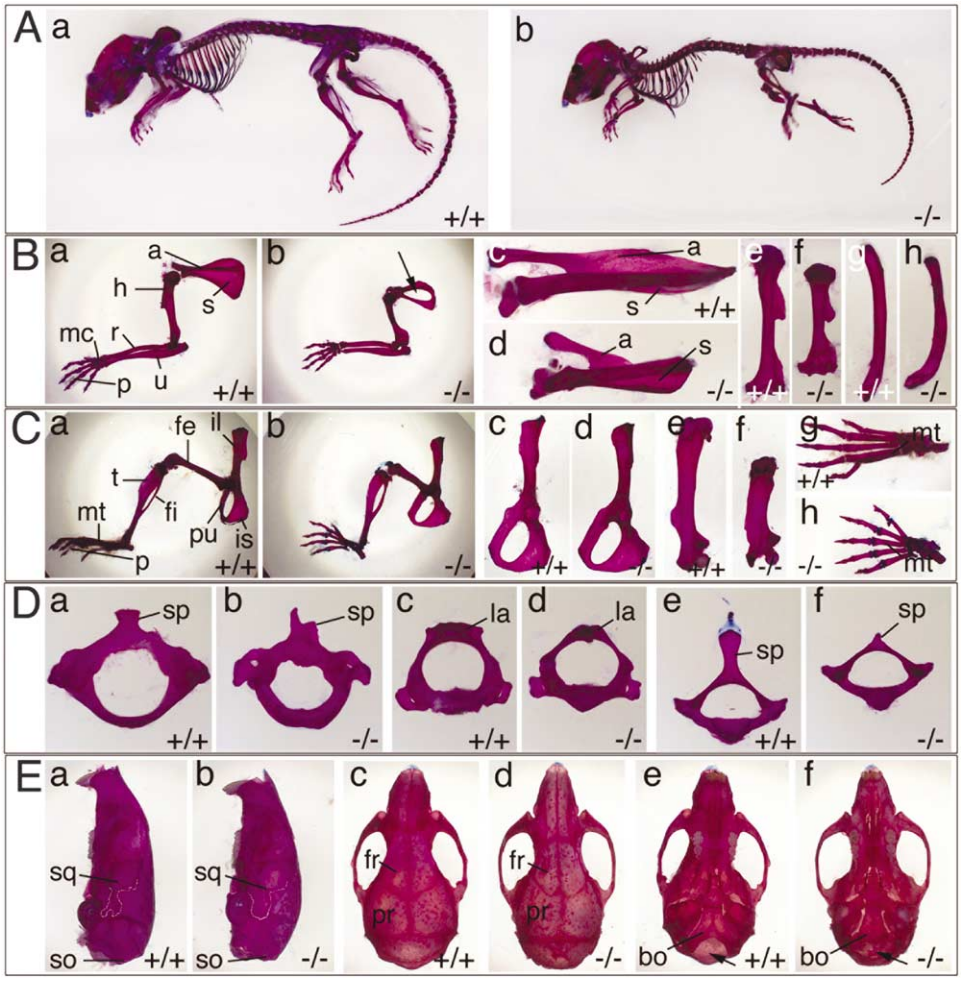

Fig. 3. Skeletal defects of adult mice mutant for *Tbx15*. Alizarin red and alcian blue stainings for ossified and chondrified parts, respectively, of skeletons of 6-week-old wildtype and *Tbx15*$^{-/-}$ mice. Genotypes are indicated in the figure. (A) Whole skeleton. (B) Forelimb and pectoral girdle preparations, (a,b) whole region, (c,d) scapula, (e,f) humerus, (g,h) clavicula. a, acromion; h, humerus; m, metacarpals; p, phalanges; r, radius; s, blade of scapula; u, ulna. (C) Hindlimb and pelvic girdle preparations, (a,b) whole region, (c,d) pelvis, (e,f) femur, (g,h) foot. fe, femur; fi, fibula; il, ileum; is, ischium; mt, metatarsals; p, phalanges; pu, pubis; t, tibia. (D) Vertebra preparations, (a,b) first cervical vertebra, atlas, (c,d) second cervical vertebra, axis, (e,f) second thoracic vertebra. la, lamina; sp, spinal process. (E) Skull preparations, (a,b) lateral view, (c,d) dorsal view, (e,f) ventral view. bo, basioccipital bone; fr, frontal bone; pr, parietal bone; so, supraoccipital bone; sq, os squamosum. Labeling is done on wildtype preparations but also applies to the mutant directly to the right. Specific changes in the mutant are highlighted by arrows and arrowheads as mentioned in the text.

The humerus is shorter and a hole is present in the scapular blade (arrow in Fig. 4Bf), the atlas is separated from the axis (arrow in Fig. 4Bg) and its ventral extension is split (arrow in Fig. 4Bg), the posterior edge of the basioccipital bone appears rugged (arrow in Fig. 4Bh).

2.5. Delay of endochondral bone development in Tbx15 mutant embryos

To determine the spatio-temporal and molecular requirements of *Tbx15* in endochondral bone formation, we analyzed the development of the humerus, a bone that appears strongly reduced in size in the mutant, using morphometric, histological and molecular analyses (Fig. 5). At E13.5, the length of the *Tbx15* mutant humerus reaches 88% of that of the wildtype. During further bone development (E15.5, E18.5, 3 months) the mutant humerus is further reduced to 83, 81% and a final 73.5%, respectively, of that of the wildtype control (Fig. 5Ae–i). This suggests that *Tbx15* is required for patterning of the mesenchymal template but may also act during further development of the cartilaginous bone, a role compatible with expression of *Tbx15* in prehypertrophic chondrocytes (Fig. 1Q,R). Histological analysis of a longitudinal section of the humerus at E15.5, 16.5 and 18.5 revealed a normal spatial pattern of chondrocyte differentiation during endochondral bone development in the mutant (Fig. 5Bg and data not shown). This was confirmed by analysis of marker gene expression for chondrocyte differentiation at E15.5 (Fig. 5Bb–e,h–k) and at E16.5 (data not shown). *Collagen II* expression marks prehypertrophic chondrocytes (Ng et al., 1993). Expression levels of *Collagen II* between

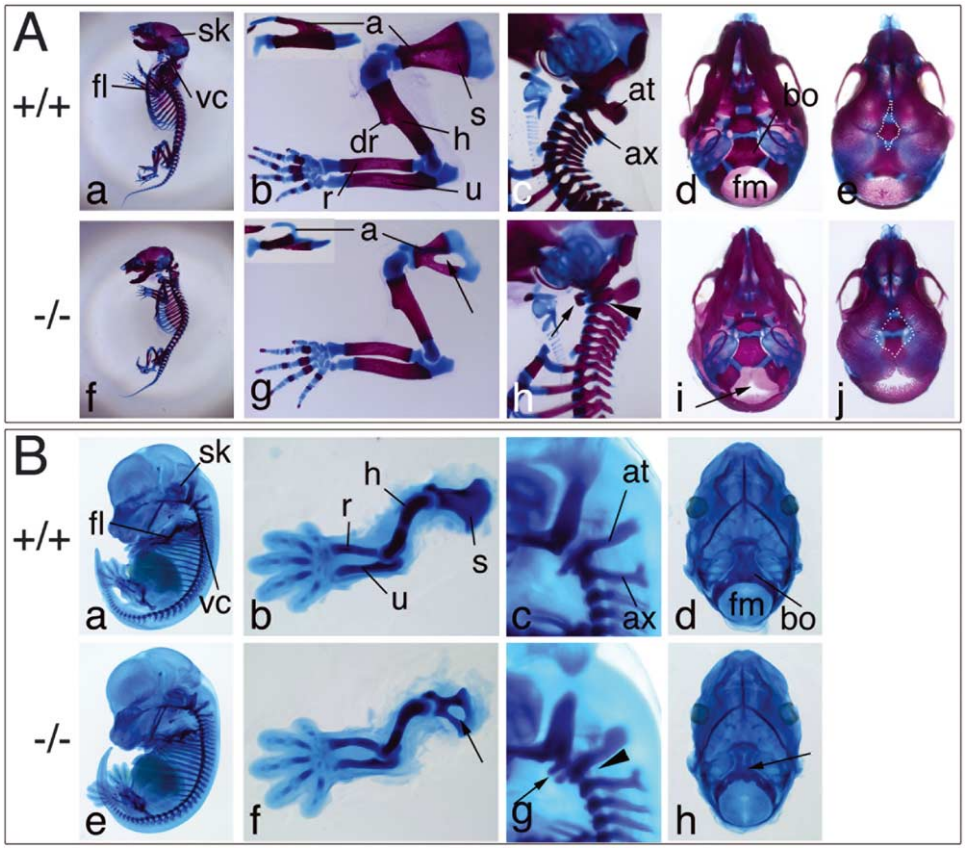

Fig. 4. Defects of skeletal development in *Tbx15*$^{-/-}$ embryos. Alizarin red and alcian blue stainings for ossified and chondrified parts, respectively, of the developing skeleton at E18.5 (A), Alcian blue staining only for cartilaginous preskeletons at E13.5 (B). Wildtype (+/+) and *Tbx15* mutants (−/−) are shown in lines as indicated. Row one shows whole skeletons (Aa,f,Ba,e), with parts labeled for higher magnification in the consecutive rows. Forelimb/pectoral girdle preparations in row two (Ab,g,Bb,f), preparations of cervical and upper thoracic parts of the vertebral column are in row three (Ac,h,Bc,g), ventral views of skulls in row four (Ad,i,Bd,h), dorsal view of skulls in row five (Ae,j). Labeling is done on wildtype preparations but also applies to the mutant directly underneath. Arrows and arrowheads as mentioned in the text highlight specific changes in the mutant. a, acromion; at, atlas; ax, axis; bo, basioccipital bone; dr, deltoid ridge of humerus; fl, forelimb/pectoral girdle; fm, foramen magnum; h, humerus; r, radius; s, blade of scapula; sk, skull; u, ulna; vc, vertebral column (cervical/upper thoracic region).

wildtype and mutants were indistinguishable. However, the total number of positive cells is reduced in *Tbx15*$^{-/-}$ embryos (Fig. 5Bb,h). *Collagen X* expression is found in hypertrophic chondrocytes (Iyama et al., 1991). Differentiation of prehypertrophic to hypertrophic chondrocytes occurs normally as shown by normal expression of *Collagen X* in the mutant (Fig. 5Bi). Ihh and PTHrP are components of a signaling system controlling chondrocyte proliferation and differentiation (for a review see Kronenberg and Chung, 2001). *Ihh* expression in late prehypertrophic and early hypertrophic chondrocytes (Fig. 5Bd,j) and *PTHrPreceptor* (*PTR*) expression in late prehypertrophic chondrocytes and in the perichondrium (Bitgood and McMahon, 1995; Karperien et al., 1994) were unchanged in the mutant humerus at E15.5 (Fig. 5Be,k). Von Kossa staining marks calcification of bones, i.e. onset of osteogenesis. The ossified domain was reduced in length in the mutant but calcification levels appeared normal (Fig. 5Bl and data not shown). Thus, chondrocyte differentiation and osteogenesis occur normally during endochondral bone development in the mutant excluding a direct role of *Tbx15* in these processes.

Growth of the cartilaginous template is primarily dependent on proliferation of chondrocytes prior to chondrocyte hypertrophy. Reduction of the number of prehypertrophic chondrocytes in the *Tbx15*$^{-/-}$ humerus at E15.5 may indicate increased apoptosis or reduced proliferation of prehypertrophic chondrocytes. To address whether loss of *Tbx15* affects programmed cell death in prehypertrophic chondrocytes, we analyzed apoptosis in wildtype and mutant embryos (Fig. 5Ca,b). Analysis of the humerus at E15.5 did not reveal any differences in apoptosis between mutant and wildtype in prehypertrophic chondrocytes at this stage. However, proliferation in *Tbx15* mutants was significantly reduced (Fig. 5Cc–e). Proliferation rates as detected by the BrdU labeling index in the humerus at E15.5 were 0.18 (s.d. 0.0025) in the wildtype but 0.161 (s.d. 0.0018) in the *Tbx15* mutant.

Alizarin/alcian preparations of developing bones have revealed a delay in endochondral ossification at early fetal stages (Fig. 5Af). Hematoxylin–eosin and van Kossa staining of

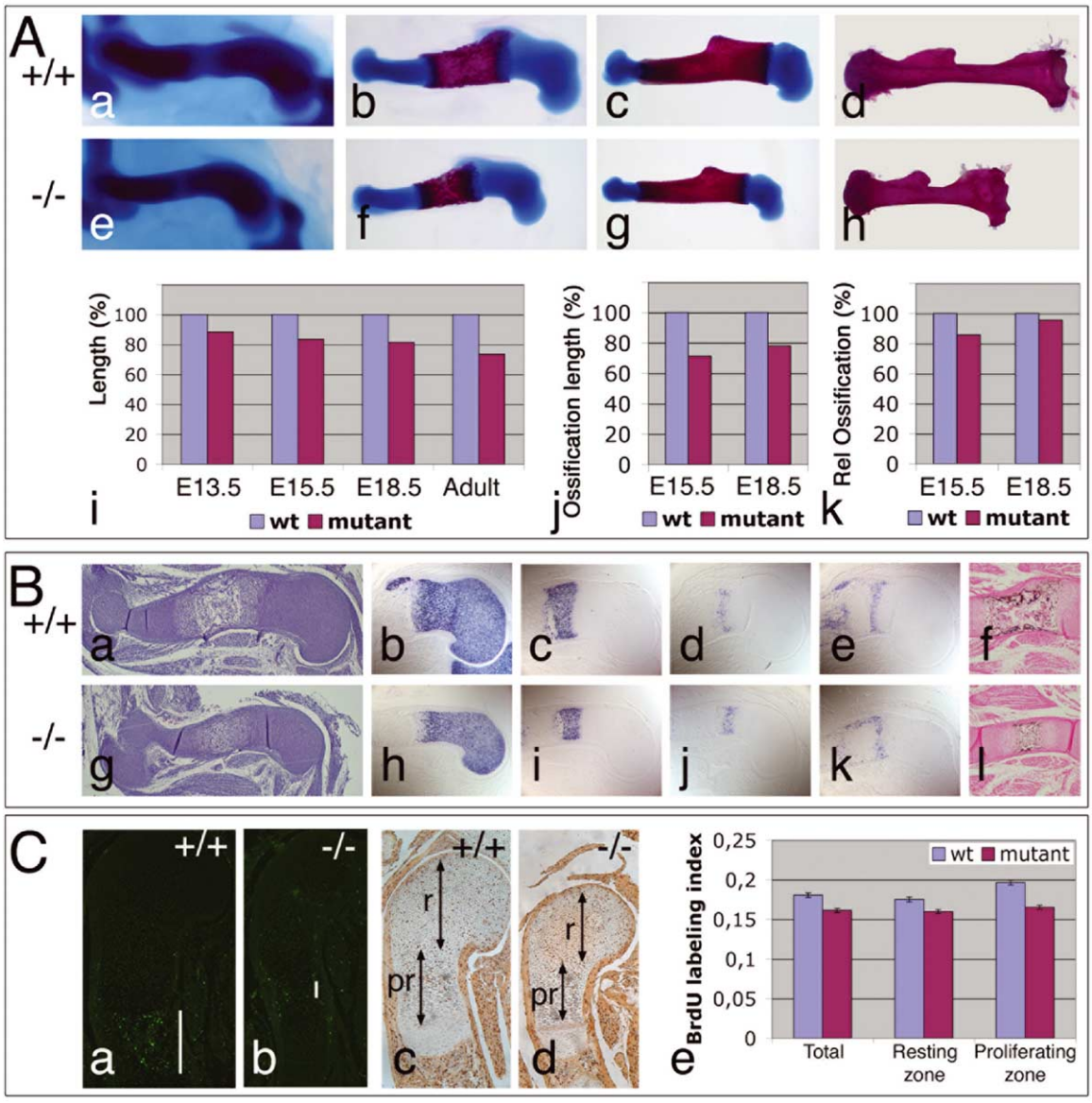

Fig. 5. Retarded endochondral development of *Tbx15* mutant humerus. (A) Morphometric analysis of bone growth and ossification in *Tbx15*$^{-/-}$ embryos. (a–h) Alcian blue/alizarin red preparations of humerus of wildtype (+/+) and *Tbx15* mutant (−/−) embryos at E13.5 (a,e), E15.5 (b,f), E18.5 (c,g) and in adult mice (d,h). The distal ends of the humeri are aligned on the left to illustrate the size differences. (i) Graphical representation of the length differences of wildtype and mutant humerus at embryonic and adult stages. Wildtype is defined as 100%. Values at E13.5 are for wildtype ($n=5$) 100±2.95%, for mutant ($n=5$) 88.4±2.65%, $P<0.00015$; at E15.5 for wildtype ($n=6$) 100±1.81%, for mutant ($n=6$) 83.4±1.8%, $P<0.0003$; at E18.5 for wildtype ($n=4$) 100±0.8%, for mutant ($n=4$) 81±1%, $P<0.00013$; in adults for wildtype ($n=4$) 100±0.82%, and for mutant ($n=4$) 73.5±1.7%, $P<0.00035$. (j) Graphical representation of the length of the ossified zone (alizarin red positive) of the humerus at E15.5 and 18.5. Wildtype is defined as 100%. Values are at E15.5 for wildtype ($n=6$) 100±5.1%, for mutant 71.3±4.6%, $P<0.00012$; at E18.5 for wildtype ($n=4$) 100±1.6%, for mutant ($n=4$) 78.1±1.6%, $P<0.00052$. (k) Graphical representation of relative ossification (alizarin red zone to total humerus length) at E15.5 and 18.5. Wildtype is defined as 100%. Values are at E15.5 for wildtype ($n=6$) 100±3.7%, for mutant ($n=6$) 85.7±4%, $P<0.00025$; at E18.5 for wildtype ($n=4$) 100±1.1%, for mutant ($n=4$) 95.6±1.8%, $P<0.00025$. (B) Histological and molecular analysis of chondrogenesis and ossification in wildtype (+/+) and *Tbx15* mutant (−/−) humerus at E15.5. (a,g) Hematoxylin–eosin staining of whole humerus, (b–e,h–k) section in situ hybridization analysis for *CollagenII* (b,h), *CollagenX* (c,i), *Ihh* (d,j) and *PTR* (e,k) expression, (f,l) van Kossa staining. (C) Analysis of apoptosis and proliferation on the proximal part of the humerus at E15.5. (a,b) TUNEL assay for apoptotic cells. White lines indicate the extension of the ossification zone in which normal apoptosis of hypertrophic chondrocytes is seen. (c,d) BrdU in vivo labeling, respectively, on sections of proximal humerus halves. (e) BrdU incorporation calculated as BrdU-positive nuclei in cartilage of proximal humerus halves at E15.5. Bars represent means± SD. Total refers to the sum of resting and proliferating chondrocytes, i.e. prehypertrophic chondrocytes. Values are for resting chondrocytes in the wildtype ($n=5$) 0.175±0.0020, and in the mutant ($n=5$) 0.159±0.0023, $P<0.00084$, for proliferating chondrocytes in the wildtype 0.196±0.0038, in the mutant 0.165±0.0027, $P<0.0005$, for total of prehypertrophic chondrocytes in the wildtype 0.180±0.0025, in the mutant 0.161±0.00175, $P<0.00073$. Prehypertrophic are the sum of resting (r) and proliferating (pr) chondrocytes.

E15.5 humerus confirmed the reduction of the ossified region at this stage (Fig. 5Bg,l). Quantitative analysis showed that the length of the ossified region is reduced to 71% of that of the wildtype at E15.5. At E18.5, the Alizarin positive region reaches 78% of the wildtype length (Fig. 5Aj). The relative ossification (defined as the length of the ossified region to the total humerus length) is 85% of that of the wildtype at E15.5, but increases to 96% of that of the wildtype at E18.5 (Fig. 5Ak).

Thus, the reduced growth of cartilaginous templates in *Tbx15*$^{-/-}$ may be caused by reduced proliferation of prehypertrophic chondrocytes. The transient delay of ossification at early embryonic stages may be secondary to the reduction (immaturity) of the overall template.

2.6. Mesenchymal precursor cells of the skeleton are affected in Tbx15 mutant embryos

A possible role for *Tbx15* in mesenchymal precursor cells of skeletal elements is suggested by the reduced size of cartilaginous templates at E13.5 in the mutant. To evaluate such an early requirement for *Tbx15*, we performed histological and marker analyses on the forelimb bud between E12.5 and 10.5. At this time mesenchymal cells have formed condensations and are beginning to aggregate, respectively (Fig. 6).

Sox9 is a marker for (and regulator of) prechondrogenic condensations (Wright et al., 1995; Akiyama et al., 2002).

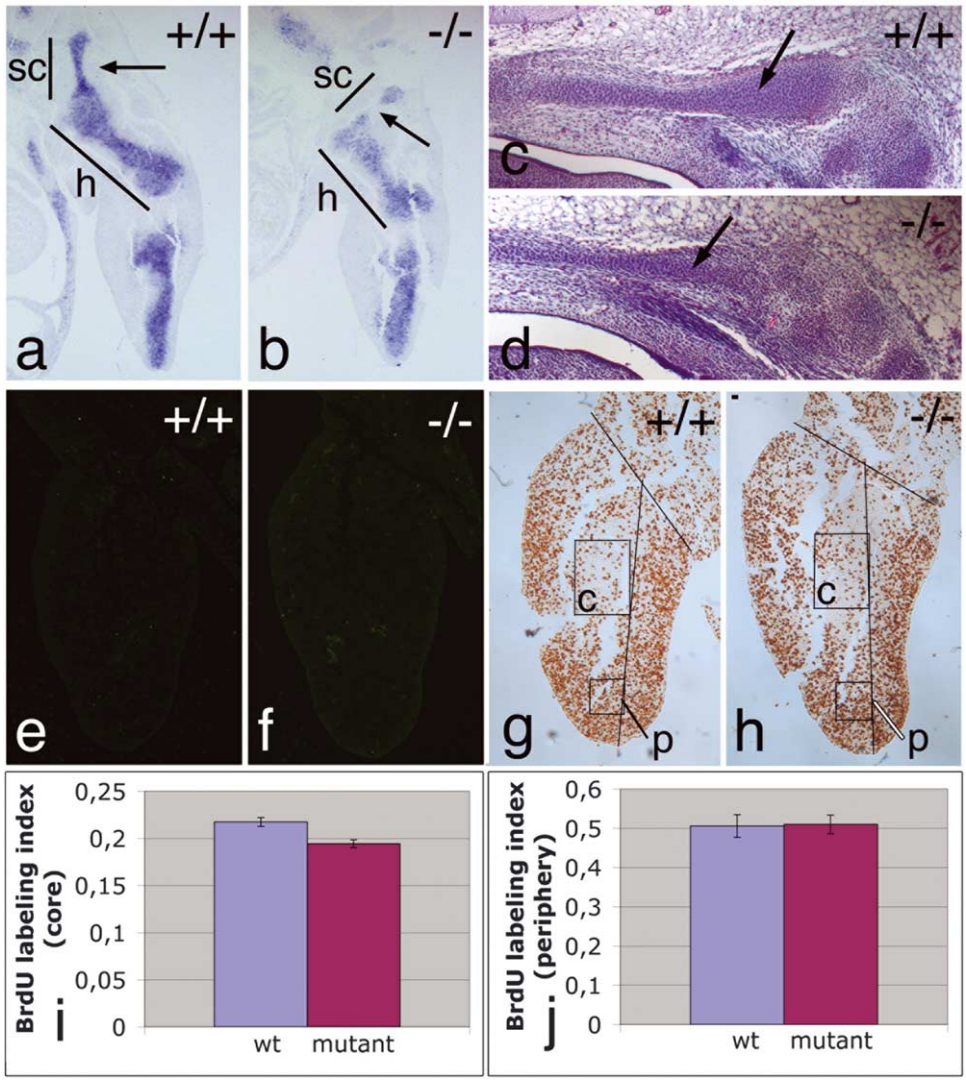

Fig. 6. Mesenchymal precursors of the skeleton are affected in *Tbx15* mutants. (a,b) Analysis of *Sox9* expression in E12.5 forelimb buds of wildtype (a) and *Tbx15*$^{-/-}$ embryos (b). Bars indicate the extension of the scapula (sc) and the humerus (h), respectively. Arrows point to the center of the scapular blade. (c,d) Hematoxylin–eosin stainings of sections of E12.5 wildtype (c) and *Tbx15*$^{-/-}$ (d) embryos in the region of the condensation of the basioccipital bone (arrows). (e,f) TUNEL assay for apoptotic cells in sections of forelimb buds of E10.5 wildtype (e) and *Tbx15*$^{-/-}$ embryos (f). (g,h) BrdU in vivo labeling on sections of forelimb buds of E10.5 wildtype (g) and *Tbx15*$^{-/-}$ embryos (h). Squares indicate the core (c) and the peripheral regions (p), respectively, used for calculating the BrdU labeling indeces. (i,j) BrdU labeling indeces calculated as ratio of BrdU-positive nuclei to total nuclei number in the core region (i) and in the peripheral region (p), respectively, of transverse sections of forelimb buds of wildtype (wt) and *Tbx15*$^{-/-}$ (mutant) embryos. Bars represent means $\pm$ SD. Values are in the core region for wildtype ($n=3$) 0.217 ± 0.0048, for the mutant ($n=3$) 0.194 ± 0.0041, $P < 0.00016$, for the periphery in the wildtype 0.505 ± 0.03, for the mutant 0.509 ± 0.024, $P = 0.8$.

At E12.5, the mesenchymal condensation of the humerus in the forelimb bud appears reduced in size in the mutant (Fig. 6b). *Sox9* expression in the center of the future scapula is missing (arrow in Fig. 6b). Similarly, histological analysis at E12.5 showed a smaller mesenchymal template of the basioccipital bone in the mutant (arrow in Fig. 6d). Smaller mesenchymal condensations may be caused by several processes including changes of adhesive properties, increased apoptosis and reduced proliferation of mesenchymal precursor cells, respectively. To address whether loss of *Tbx15* affects programmed cell death in mesenchymal precursor cells, we analyzed apoptosis in wildtype and mutant embryos (Fig. 6e,f). Analysis of forelimb buds at E10.5 did not reveal any differences in apoptosis between wildtype and mutant. *Tbx15* is highly expressed in the core of the E10.5 forelimb bud but can only be weakly detected in peripheral regions. Proliferation in the core region of the limb bud as judged by the BrdU labeling index was significantly reduced from 0.217 ± 0.0048 in the wildtype to 0.194 ± 0.0041 in the mutant ($P < 0.00016$) (Fig. 6g–i). In contrast, proliferation in the peripheral region was found to be unchanged (0.51 ± 0.03 in the wildtype vs 0.51 ± 0.024 in the mutant, $P = 0.8$ (Fig. 6j). This suggests reduced size of condensations and subsequent skeletal defects may be partly attributed to a reduced number of mesenchymal precursor cells.

2.7. Tbx15 and early limb patterning

Tbx15 expression is high in the proximal core but low in the distal mesenchyme, including the progress zone. Along the anterior–posterior axis expression is excluded from the flanks and future digits I and V (Figs. 1B,F,P, 2Cc). The severity of the defects in the mutant forelimb skeleton appears higher in the proximal (pectoral girdle and stylopodium) than in the distal region (zeugopodium and autopodium) suggesting a function of *Tbx15* in patterning proximal skeletal elements in the limb. However, expression of various signaling molecules and transcription factors critical for limb patterning such as *Wnt7a* (Parr and McMahon, 1995), *Shh* (Riddle et al., 1993), *Fgf8* (Mahmood et al., 1995), *Meis1* and *Meis2* (Nakamura et al., 1996), members of subgroups 9–13 of the *HoxA* and *HoxD* clusters (Zákány and Duboule, 1999) as well as *Cart1, Prx1, Prx2, Alx3* and *Alx4* (Lu et al., 1999; Takahashi et al., 1998), *Emx2* (Pellegrini et al., 2001), *Pax1* (Wilm et al., 1998) were unaltered in *Tbx15* mutants (data not shown).

Likewise, expression of other *Tbx* genes, transcribed during limb development, were unaffected in *Tbx15* mutants (data not shown).

3. Discussion

The size, shape and position of each bone in the vertebrate skeleton depend both on patterning processes acting on mesenchymal precursor cells and on differentiation of these precursor cells along the chondrogenic and osteogenic lineages. This study shows that *Tbx15*, a T-box transcription factor, regulates skeletal development both at the level of mesenchymal precursor cells and chondrocytes by maintaining an appropriate rate of cell proliferation. Recently, it was shown that the *droopy ear* mutation of the mouse is caused by a deletion of the *Tbx15* gene (Candille et al., 2004). Our analysis of the phenotype of an engineered null allele of *Tbx15* confirms the description of the *droopy ear* skeletal phenotype (Curry, 1959). It extends this analysis by defining the spatio-temporal and molecular requirements for *Tbx15* during early skeletal development.

3.1. Tbx15 and skeletal development

Tbx15$^{-/-}$ mice display defects in specific elements of the appendicular skeleton, the vertebral column and the head skeleton including the skull affecting both bones developing by intramembranous as well as endochondral ossification. Defects in bones developing by either pathway may be explained by a role of *Tbx15* in the proliferation, aggregation and condensation of mesenchymal precursor cells and/or a later function in chondrogenesis and osteogenesis, respectively, of the mesenchymal preskeleton. We favor the idea that *Tbx15* acts primarily during mesenchymal stages of skeletogenesis and in early cartilaginous templates for the following reasons.

Tbx15 is strongly expressed in the mesenchymal core of the developing limb bud, in the cranial paraxial mesoderm and in supraocular mesenchyme. Proliferation in the region of high *Tbx15* expression in the mesenchymal core of the forelimb bud is reduced by 10% compared to the wildtype. It appears that mesenchymal condensations form at specific stages of limb development irrespective of the number of progenitor cells present. If the timing of condensations is fixed then a reduction in cell number should result in smaller and misshapen prechondrogenic templates. If the cell number drops below a certain threshold condensations do not develop (Wolpert et al., 1979; Yamaguchi et al., 1999). Thus, the small but significant reduction in proliferation of mesenchymal progenitor cells in *Tbx15* mutants is compatible with the presence of smaller templates in the mesenchymal preskeleton at E12.0–12.5. In case of the scapular blade, a sufficiently high cell number to initiate condensation is never achieved leading to a hole in the central part of the blade. Increased adhesion of mesenchymal cells is another requirement for aggregation and condensation of these cells. At this point we cannot exclude that *Tbx15* additionally regulates adhesion properties of mesenchymal cells.

Reduced proliferation but apparently normal differentiation of prehypertrophic chondrocytes in *Tbx15* mutant mice argues for a cell-autonomous function of this transcription factor in maintaining the appropriate cell number in this compartment. Weak expression of *Tbx15* in

prehypertrophic chondrocytes and rapid downregulation of expression after E16.5 in cartilaginous templates support the notion that *Tbx15* plays only a transient and minor role in early endochondral bone formation.

We did not detect expression of *Tbx15* in osteoblasts during intramembranous bone development of flat bones of the skull. Thus, slight changes of shape of skull bones in *Tbx15* mutants (e.g. of the os squamosum) might be attributed to defects in mesenchymal precursor cells.

At this point the molecular pathways regulated by *Tbx15* are unknown. The small but significant reduction of proliferation in limb bud mesenchyme suggests that Tbx15 intersects with the cell cycle machinery either by transcriptionally repressing cell cycle inhibitors or activating cell cycle activators.

It is well known that the skeleton and the skeletal musculature of adult vertebrates constitute a system in which the two components mutually depend on each other. Reduction of muscle mass leads to reorganization of the bone matrix. Degradation of bones leads to muscle weakness. *Tbx15* is expressed both in developing bones and the skeletal musculature. However, expression in skeletal muscles is only detected from E13.5 onwards. Differentiation of muscles occurs normally in the mutant but muscle mass appears reduced at E18.5 (Singh et al., unpublished observations). In contrast, the skeletal phenotype was traced back to proliferation defects from E10.5 onwards. Hence, we assume that the skeletal phenotype is largely independent from a requirement for *Tbx15* in skeletal muscle development.

3.2. Tbx15 and limb patterning

Tbx15 expression extends along the PD-axis of the limb bud with a strong expression in the central region, and is excluded from the anterior and posterior flanks with future digits I and V suggesting a function in patterning these axes. Analyses of mutant appendicular skeletons as well as of molecular marker expression do not support such a role, although we cannot exclude that subtle changes were unnoticed. Conceivably, the relatively mild skeletal phenotype of *Tbx15* mutant limbs reflects redundancy with the closely related T-box gene, *Tbx18*. Within the T-box, sequence conservation amounts to 93% (Kraus et al., 2001). This suggests that *Tbx15* and *Tbx18* might have the same DNA binding specificity, thus, share molecular targets. *Tbx18*$^{-/-}$ mice do not show a limb phenotype although the gene is strongly expressed in the proximal part of the limb bud mesenchyme (Bussen et al., 2004). Double mutant analysis will reveal a redundant function of this closely related pair of T-box genes in patterning the limb skeleton.

Tbx15 expression completely or partially overlaps also with that of members of other subfamilies of T-box transcription factors. Compound mutants of *Tbx15* with other *Tbx* genes expressed during limb development (*T*, *Tbx2*, *Tbx3*, *Tbx4* and *Tbx5*) as well as biochemical analysis of DNA-binding properties of these transcription factors will help to unravel the functional specificity and interaction of *Tbx* genes in vertebrate limb development.

4. Experimental Procedures

4.1. Isolation and characterization of a Tbx15 cDNA

To identify new members of the murine T-box gene family we searched the dbEST library with several known T-box motifs. One EST clone (AA027675) was found to encode a short stretch of a novel mouse T-box protein. The 0.5 kbp cDNA insert was used as a probe to screen cDNA plasmid libraries prepared from RNA of 9.5 and 12.5-day embryos (obtained from the Resourcenzentrum in Berlin). One positive clone was purified and the 3.5 kbp cDNA insert fully sequenced. Sequence comparison confirmed identity with published cDNA sequences deposited in the databases as *Tbx15* (AF041822, Agulnik et al., 1998) and *Tbx15/Tbx14* (NM_011534, Wattler et al., 1998). The full-length sequence of our mouse *Tbx15* cDNA was deposited in the GeneBank database under the accession number AY662679.

4.2. Generation of Tbx15 mutant mice

To clone the mouse *Tbx15* locus a 129/Ola genomic phage library was screened using the mouse cDNA as a probe. Nine independent phage clones were purified. A 15.5 kbp *Not*I-fragment harboring the T-box-region of the *Tbx15* transcription unit was subcloned from one of them and characterized by restriction and exon mapping. A *Bam*HI-site in the third exon which encodes a part of the 5′-region of the T-box was replaced by an *Nco*I-site allowing an in frame insertion of the *lacZ* gene. The *lacZ* gene was followed by a loxP-flanked *neo*-cassette, and flanked by two homology regions of approximately 2 and 7.5 kbp, respectively, derived from the *Not*I-subfragment (Fig. 2A). This *lacZ* insertion vector should ensure the generation of a null allele and allow monitoring expression of the *Tbx15* locus by the β-galactosidase activity assay (Fig. 2D). The targeting vector was linearized at a unique *Sal*I-site and electroporated in ES cells of 129/Ola genotype. 54 G418 resistant ES cell clones were screened for homologous recombination in the *Tbx15* locus by Southern blot analysis. Eight ES cell clones (of 17 with homologous recombination) were positively rescreened and were subsequently used for microinjection into NMRI mouse blastocysts. Three chimeric males were obtained and mated to NMRI females. One chimera gave germ line transmission. F1 heterozygous males were crossed to NMRI females, heterozygous offspring intercrossed and embryos and newborns analyzed for phenotypic alterations.

4.3. Genotyping of Tbx15 mutant mice

Genotypic characterization of ES cells, embryos and adult mice was done by Southern blot analysis of restriction digested genomic DNA. DNA was derived from ES cells, embryonic yolk sacs and from adult tails, and hybridized with probes distinguishing wild type and mutant alleles (Fig. 2A). The 5′-probe is a 1.2 kbp *Not*I-*Nco*I-fragment from the genomic region adjacent but outside the targeting vector. This probe recognizes a 4 kbp *Bam*HI-fragment in the wildtype and a 7 kbp *Bam*HI-fragment in the mutant (Fig. 2B). The *neo*-probe was used to analyze the single nature of the integration event.

In addition, a PCR protocol was established to speed up genotyping of *Tbx15* heterozygous mice. Primers 581 (sense: 5′-CAGCCGCTACAGTCAACAG) and 354 (antisense: 5′-CCGGCTTTGGTGATGATC) amplify a 1800 bp fragment from the *Tbx15* mutant allele (Fig. 2A,C).

4.4. Histological analysis

Embryos for histological analysis were fixed in Bouin's fixative, paraffin embedded and sectioned to 5–10 μm. Sections were stained with hematoxylin and eosin. For van Kossa stainings 10 μm sections were deparaffinized and rehydrated. They were then incubated in 5% silver nitrate solution for 1 h in front of a 60-W lamp. Sections were rinsed three times with distilled water, incubated in 5% sodium thiosulphate for 5 min, washed with distilled water and counterstained with Nuclear Fast Red for 5 min. Sections were rinsed, dehydrated and mounted with Permount. Histochemistry for β-galactosidase was carried out as described (Echelard et al., 1994).

4.5. Skeletal preparations of embryos and mice

Skeletal preparations of embryos, newborns and adults were performed as previously described (Mallo and Brändlin, 1997; Bussen et al., 2004).

4.6. Proliferation and apoptosis assays

Cell proliferation in limbs of E10.5 and 15.5 embryos was investigated by detection of incorporated BrdU similar to published protocols (Mansouri et al., 2000; Bussen et al., 2004). Three to four embryos of each genotype and stage were used in this study; at least three sections of each genotype and stage were analyzed. At E10.5, transverse sections of limb buds were analyzed, BrdU-positive cells were counted in the center and periphery of the limb bud, respectively, as shown in Fig. 6 g,h. At E15.5, longitudinal sections through the humerus were used. BrdU-positive cells were counted in the proximal part of humerus. The chondrocyte region was divided into two zones before hypertrophy. The resting zone, which is adjacent to the joint, is composed of round cells while the proliferating zone is composed of mostly flattened and columnar chondrocytes lying adjacent to the hypertrophic chondrocytes. The BrdU-labeling rate was defined as the number of BrdU-positive nuclei relative to the total number of nuclei as detected by DAPI counterstain. The mean values and standard deviation were determined and the *Student t-test* was performed to test for statistical relevance.

For analysis of programmed cell death, 3–4 embryos of each genotype and stage were used; at least 3–4 sections of each genotype and stage were analyzed. Detection of apoptotic cells in paraffin sections of limbs of E10.5 and 15.5 embryos was based on modification of genomic DNA utilizing terminal deoxynucleotidyl transferase (TUNEL assay) and indirect detection of positive cells by Fluorescein conjugated anti-digoxigenin antibody. The procedure followed the recommendation of the manufacturer (Serologicals Corporation) of the ApopTag kit used.

4.7. In situ hybridization analysis

Whole-mount in situ hybridization was performed following a standard procedure with digoxigenin-labeled antisense riboprobes (Wilkinson, 1992). The probes used were *Alx3* and *Cart1* (ten Berge et al., 1998), *Alx4* (Qu et al., 1997), *Emx2* (Pellegrini et al., 2001), *Fgf8* (Mahmood et al., 1995), *Hoxa10, Hoxd9, Hoxd11, Hoxd12* (Zákány and Duboule, 1999 and references therein), *Meis1* and *Meis2* (Nakamura et al., 1996), *Pax1* (Deutsch et al., 1991), *Prx1* and *Prx2* (Leussink et al., 1995), *Shh* (Riddle et al., 1993), *Tbx2*, *Tbx3*, *Tbx4* and *Tbx5* (Gibson-Brown et al., 1996), *Tbx18* (Kraus et al., 2001), *Wnt7a* (Parr and McMahon, 1995). A *Tbx15*-specific riboprobe was generated from the 3.7 kbp cDNA subcloned in pBluescriptIIKS (Stratagene) using T3 RNA polymerase after linearization with *Sac*II. Stained specimens were transferred in 50% glycerol prior to documentation.

In situ hybridization analysis on 10 μm paraffin sections was done essentially as described (Lescher et al., 1998). The probes used were *CollagenII* (Ng et al., 1993), *CollagenX* (Iyama et al., 1991), *Ihh* (Bitgood and McMahon, 1995), *PTR* (Karperien et al., 1994), and *Sox9* (Wright et al., 1995).

4.8. Documentation

Whole-mount specimens were photographed on Leica M420 with Fujix digital camera HC-300Z, sections on Leica Axioplan with ProgResC14 digital camera. All images were processed in Adobe Photoshop 7.0.

Acknowledgements

We thank Achim Gossler for discussion and critical reading of the manuscript, Rudi Balling, Denis Duboule, Frits Meijlink, Ahmed Mansouri, Andy McMahon, Eric Olson, Virginia Papaioannou and Shinji Takada for probes, Rolf Kemler and the Max-Planck-Society for support. The 129/Ola cosmid genomic and the cDNA libraries were obtained from

the Resourcenzentrum (RZPD) in Berlin. This work was supported by a grant of the German Research Foundation to A.K. (DFG KI728/3).

References

Agulnik, S.I., Papaioannou, V.E., Silver, L.M., 1998. Cloning, mapping, and expression analysis of TBX15, a new member of the T-Box gene family. Genomics 51, 68–75.

Akiyama, H., Chaboissier, M.C., Martin, J.F., Schedl, A., de Crombrugghe, B., 2002. The transcription factor Sox9 has essential roles in successive steps of the chondrocyte differentiation pathway and is required for expression of Sox5 and Sox6. Genes Dev. 16, 2813–2828.

Bamshad, M., Lin, R.C., Law, D.J., Watkins, W.C., Krakowiak, P.A., Moore, M.E., et al., 1997. Mutations in human TBX3 alter limb, apocrine and genital development in ulnar-mammary syndrome. Nat. Genet. 16, 311–315.

Bitgood, M.J., McMahon, A.P., 1995. Hedgehog and Bmp genes are coexpressed at many diverse sites of cell–cell interaction in the mouse embryo. Dev. Biol. 172, 126–138.

Bussen, M., Petry, M., Schuster-Gossler, K., Leitges, M., Gossler, A., Kispert, A., 2004. The T-box transcription factor Tbx18 maintains the separation of anterior and posterior somite compartments. Genes Dev. 18, 1209–1221.

Candille, S.I., Raamsdonk, C.D., Chen, C., Kuijper, S., Chen-Tsai, Y., Russ, A., et al., 2004. Dorsoventral patterning of the mouse coat by tbx15. PLoS Biol. 2, 30–42.

Curry, G.A., 1959. Genetical and developmental studies on droopy-eared mice. J. Embryol. Exp. Morphol. 7, 39–65.

Davenport, T.G., Jerome-Majewska, L.A., Papaioannou, V.E., 2003. Mammary gland, limb and yolk sac defects in mice lacking Tbx3, the gene mutated in human ulnar mammary syndrome. Development 130, 2263–2273.

Deutsch, U., Dressler, G.R., Gruss, P., 1991. Pax1, a member of a paired box homologous murine gene family, is expressed in segmented structures during development. Cell 53, 617–625.

Echelard, Y., Vassileva, G., McMahon, A.P., 1994. Cis-acting regulatory sequences governing Wnt-1 expression in the developing mouse CNS. Development 120, 2213–2224.

Gibson-Brown, J.J., Agulnik, S.I., Chapman, D.L., Alexiou, M., Garvey, N., Silver, L.M., Papaioannou, V.E., 1996. Evidence of a role for T-box genes in the evolution of limb morphogenesis and the specification of forelimb/hindlimb identity. Mech. Dev. 56, 93–101.

Iyama, K., Ninomiya, Y., Olsen, B.R., Linsenmayer, T.F., Trelstad, R.L., Hayashi, M., 1991. Spatiotemporal pattern of type X collagen gene expression and collagen deposition in embryonic chick vertebrae undergoing endochondral ossification. Anat. Rec. 229, 462–472.

Karperien, M., Van Dijk, T.B., Hoeijmakers, T., Cremers, F., Abou-Samra, A.B., Boonstra, J., et al., 1994. Expression pattern of parathyroid hormone/parathyroid hormone related peptide receptor mRNA in mouse postimplantation embryos indicates involvement in multiple developmental processes. Mech. Dev. 47, 29–42.

Karsenty, G., Wagner, E.F., 2002. Reaching a genetic and molecular understanding of skeletal development. Dev. Cell 2, 389–406.

Kraus, F., Haenig, B., Kispert, A., 2001. Cloning and expression analysis of the mouse T-box gene Tbx18. Mech. Dev. 100, 83–86.

Kronenberg, H.M., 2003. Developmental regulation of the growth plate. Nature 423, 332–336.

Kronenberg, H.M., Chung, U., 2001. The parathyroid hormone-related protein and Indian hedgehog feedback loop in the growth plate. Novartis Found. Symp. 232, 144–152.

Lescher, B., Haenig, B., Kispert, A., 1998. sFRP-2 is a target of the Wnt-4 signaling pathway in the developing metanephric kidney. Dev. Dyn. 213, 440–451.

Leussink, B., Brouwer, A., el Khattabi, M., Poelmann, R.E., Gittenberger-de Groot, A.C., Meijlink, F., 1995. Expression patterns of the paired-related homeobox genes MHox/Prx1 and S8/Prx2 suggest roles in development of the heart and the forebrain. Mech. Dev. 52, 51–64.

Li, Q.Y., Newbury-Ecob, R.A., Terrett, J.A., Wilson, D.I., Curtis, A.R., Yi, C.H., et al., 1997. Holt-Oram syndrome is caused by mutations in TBX5, a member of the Brachyury (T) gene family. Nat. Genet. 15, 21–29.

Liu, C., Nakamura, E., Knezevic, V., Hunter, S., Thompson, K., Mackem, S., 2003. A role for mesenchymal T-box gene Brachyury in AER formation during limb development. Development 130, 1327–1337.

Lu, M.F., Cheng, H.T., Lacy, A.R., Kern, M.J., Argao, E.A., Potter, S.S., et al., 1999. Paired-related homeobox genes cooperate in handplate and hindlimb zeugopod morphogenesis. Dev. Biol. 205, 145–157.

Mahmood, R., Bresnick, J., Hornbruch, A., Mahony, C., Morton, N., Colquhoun, K., et al., 1995. A role for FGF-8 in the initiation and maintenance of vertebrate limb bud outgrowth. Curr. Biol. 5, 797–806.

Mallo, M., Brändlin, I., 1997. Segmental identity can change independently in the hindbrain and rhombencephalic neural crest. Dev. Dyn. 210, 146–156.

Mansouri, A., Voss, A.K., Thomas, T., Yokota, Y., Gruss, P., 2000. Uncx4.1 is required for the formation of the pedicles and proximal ribs and acts upstream of Pax9. Development 127, 2251–2258.

Mariani, F.V., Martin, G.R., 2003. Deciphering skeletal patterning: clues from the limb. Nature 423, 319–325.

Naiche, L.A., Papaioannou, V.E., 2003. Loss of Tbx4 blocks hindlimb development and affects vascularization and fusion of the allantois. Development 130, 2681–2693.

Nakamura, T., Jenkins, N.A., Copeland, N.G., 1996. Identification of a new family of Pbx-related homeobox genes. Oncogene 13, 2235–2242.

Ng, L.J., Tam, P.P., Cheah, K.S., 1993. Preferential expression of alternatively spliced mRNAs encoding type II procollagen with a cysteine-rich amino-propeptide in differentiating cartilage and nonchondrogenic tissues during early mouse development. Dev. Biol. 159, 403–417.

Niswander, L., 2003. Pattern formation: old models out on a limb. Nat. Rev. Genet. 2, 133–143.

Papaioannou, V.E., 2001. T-box genes in development: from hydra to humans. Int. Rev. Cytol. 207, 1–70.

Parr, B.A., McMahon, A.P., 1995. Dorsalizing signal Wnt-7a required for normal polarity of D–V and A–P axes of mouse limb. Nature 374, 350–353.

Pellegrini, M., Pantano, S., Fumi, M.P., Lucchini, F., Forabosco, A., 2001. Agenesis of the scapula in Emx2 homozygous mutants. Dev. Biol. 232, 149–156.

Qu, S., Niswender, K.D., Ji, Q., Van der Meer, R., Keeney, D., Magnuson, M.A., Wisdom, R., 1997. Polydactyly and ectopic ZPA formation in Alx-4 mutant mice. Development 124, 3999–4008.

Rallis, C., Bruneau, B.G., del Buono, J., Seidman, C.E., Seidman, J.G., Nissim, S., et al., 2003. Tbx5 is required for forelimb bud formation and continued outgrowth. Development 130, 2741–2751.

Riddle, R.D., Johnson, R.L., Laufer, E., Tabin, C., 1993. Sonic hedgehog mediates the polarizing activity of the ZPA. Cell 75, 1401–1416.

Rodriguez Esteban, C., Tsukui, T., Yonei, S., Magallon, J., Tamura, K., Izpisua-Belmonte, J.C., 1999. The T-box genes Tbx4 and Tbx5 regulate limb outgrowth and identity. Nature 398, 814–818.

Suzuki, T., Takeuchi, J., Koshiba-Takeuchi, K., Ogura, T., 2004. Tbx genes specify posterior digit identity through Shh and BMP signaling. Dev. Cell 6, 43–53.

Takahashi, M., Tamura, K., Buscher, D., Masuya, H., Yonei-Tamura, S., Matsumoto, K., et al., 1998. Role of Alx-4 in the establishment of anteroposterior polarity during vertebrate limb development. Development 125, 4417–4425.

Takeuchi, J.K., Koshiba-Takeuchi, K., Matsumoto, K., Vogel-Hopker, A., Naitoh-Matsuo, M., Ogura, K., et al., 1999. Tbx5 and Tbx4 genes determine the wing/leg identity of limb buds. Nature 398, 810–814.

Takeuchi, J.K., Koshiba-Takeuchi, K., Suzuki, T., Kamimura, M., Ogura, K., Ogura, T., 2003. Tbx5 and Tbx4 trigger limb initiation through activation of the Wnt/Fgf signaling cascade. Development 130, 2729–2739.

ten Berge, D., Brouwer, A., el Bahi, S., Guenet, J.L., Robert, B., Meijlink, F., 1998. Mouse Alx3: an aristaless-like homeobox gene expressed during embryogenesis in ectomesenchyme and lateral plate mesoderm. Dev. Biol. 199, 11–25.

Tickle, C., 2003. Patterning systems—from one end of the limb to the other. Dev. Cell 4, 449–458.

Wattler, S., Russ, A., Evans, M., Nehls, M., 1998. A combined analysis of genomic and primary protein structure defines the phylogenetic relationship of new members if the T-box family. Genomics 48, 24–33.

Wilkinson, D.G., 1992. Whole mount in situ hybridization of vertebrate embryos, In: Wilkinson, D.G. (Ed.), In situ Hybridization: A Practical Approach. Oxford University Press, Oxford, pp. 75–84.

Wilm, B., Dahl, E., Peters, H., Balling, R., Imai, K., 1998. Targeted disruption of Pax1 defines its null phenotype and proves haploinsufficiency. Proc. Natl Acad. Sci. USA 95, 8692–8697.

Wolpert, L., Tickle, C., Sampford, M., 1979. The effect of killing by X-irradiation on pattern formation in the chick limb. J. Embryol. Exp. Morphol. 50, 175–193.

Wright, E., Hargrave, M.R., Christiansen, J., Cooper, L., Kun, J., Evans, T., et al., 1995. The Sry-related gene Sox9 is expressed during chondrogenesis in mouse embryos. Nat. Genet. 9, 15–20.

Yamaguchi, T.P., Bradley, A., McMahon, A.P., Jones, S., 1999. A Wnt5a pathway underlies outgrowth of multiple structures in the vertebrate embryo. Development 126, 1211–1223.

Zákány, J., Duboule, D., 1999. Hox genes in digit development and evolution. Cell Tissue Res. 296, 19–25.